Fractal Attributes and Multilayer Perceptron for Agricultural Land Detection

Mohamed KHIDER[1], Soumeya OURABIA[2]

[1] University of Sciences and Technology Houari Boumediene –USTHB– Faculty of electrical engineering, Laboratory of Image Processing and Radiation Algiers, Algeria
E-mail: khider1234@gmail.com
[2] University Center of Tipaza –Morsli Abdelah-, Institut of Sciences, Departement of Electronics, Laboratory of Image Processing and Radiation –USTHB- Algeria

E-mail: s.ourabia.dz@gmail.com

Abstract **-** The present work proposes the study of parameter combinations for agricultural land detection, using the LANDSAT-8 satellite database, based on several fractal attributes and the NVDI vegetation index, followed by the evaluation of dispersion through variance analysis and using Multilayer Perceptron MLP for detection. The most robust combination for detection is then chosen. In addition, results obtained with natural textures from Brodatz are presented through fractal analysis. After Otsu binary conversion, we propose determining the fractal dimension of binary sets, as well as the dimension of their contours and area perimeter. Furthermore, we have included conventional methods such as Box-counting, fractal Lacunarity, and analysis by power spectrum.

Keywords **-** Area-Perimeter Dimension, Contour Dimension, Fractal Analysis, Fractal Lacunarity, Sets-Dimension , Spectral Analysis, MLP, NVDI.

I. INTRODUCTION

The calculation of fractal dimension applies to irregular objects that cannot be described with a single scale of measurement [1], [2]. Mandelbrot was the first to use the word "fractal", successfully establishing links between mathematical theories and real-world phenomena [3], [4]. There are several methods for estimating fractal dimension, including Box-counting, Self-similarity, Capacity, Area-perimeter, Minkowski-Bouligand, Generalized dimension, and Spectral analysis [5-10]. In this paper, we examine the potential of combining multiple fractal attributes to classify natural textures, and we introduce variance analysis to estimate dispersion. In practice, we tested 10 Brodatz textures with 6 fractal attributes. Moreover, we analyzed Landsat-8 satellite image throughout four multispectral bandsthat represent different regions using seven fractal attributes, followed by a subsequent evaluation of variance. The multispectral images play a crucial role in the detection and monitoring of agricultural and urban lands [11], [12] on a large scale. Their ability to capture a range of wavelengths of light allows for distinguishing between different land surface features, which is essential for assessing land use trends.

Then, we employed a classification method based on Multi-Layer Perceptrons (MLP) to identify agricultural land within the satellite images. Our research aligns with existing literature concerning satellite image classification techniques employing artificial neural networks [13], fractal texture analysis [14][15][16][17], and the detection of agricultural fields in satellite imagery [18].

Recent advancements in deep learning techniques have further enhanced the analysis of multispectral images. Convolutional neural networks (CNNs) have shown promising results in land cover classification tasks, providing more accurate and efficient methods for extracting information from multispectral data. By incorporating deep learning algorithms,

researchers can achieve higher classification accuracies and improve the understanding of complex spatial patterns in agricultural and urban landscapes. This work can be summarized as follows :

Extraction of Fractal Attributes: Fractal attributes are typically computed from the image to capture features related to the fractal structure.

Data Preprocessing: It is necessary to normalize and preprocess the fractal attributes appropriately to make them suitable for MLP training.

MLP Architecture: We need to define the architecture of the MLP based on the number of extracted fractal attributes and the number of classes. The input layer of the MLP has a number of neurons equal to the number of fractal attributes, and the output layer will have a number of neurons equal to the number of classes.

Loss Function and Activation: Choosing an appropriate loss function for classification and suitable activation functions for hidden layers and the output layer is essential.

Training: MLP training is performed using gradient descent optimization.

Evaluation: Evaluate the MLP model on a test dataset to measure performance in terms of precision, using the F-measure metric.

Indeed, an MLP is used for image classification with fractal attributes as inputs. It's worth noting that CNNs are also suitable for image classification as they can capture important spatial features that MLPs may not represent as effectively. However, the uniqueness of this work lies in proposing the extraction of fractal attributes followed by the use of an MLP for classification, and more precisely for agricultural land detection.

II. METHOD AND FRACTAL ATTRIBUTES

The first step is to determine the fractal attributes in order to obtain Lacunarity, contour dimension, sets dimension, and area-perimeter dimension. The image is first binarized by applying a threshold to its histogram. Processing a binary image represents a significant time gain.

The reference methods that can be cited are the Otsu method and the Kapur et al. method [19], [20] as well as the Trussell method [21], [22]. Indeed, other thresholding techniques that have emerged subsequently rely on the first two methods [23]. In this work, the Otsu method is employed. We begin by calculating the probability density of the different grayscale levels of the image. Let h be the histogram of the image, the probability density function is given by:

$$p_i = \frac{h(i)}{\sum_{j=0}^{L-1} h(j)} \tag{1}$$

$h(i)$: is the number of occurrences of the gray level pixel in the image $i \in \{1,...,L-1\}$.

p_i : the probability density function.

L : the size of the histogram.

J : the gray level.

In order to binarize, the optimal threshold t* is the one that maximizes the ratio of inter-class variance to total variance.

$$t^* = Arg\max_{th}\left(\frac{\sigma_B^{2(th)}}{\sigma_T^{2(th)}}\right) \tag{2}$$

Knowing that the parameters *th*, σ_T^2 and σ_B^2 represents repectively the threshold index, the total variance, and the interclass variance.

$$\sigma_B^{2(th)} = P_{th}(P_{th}-1)(\mu_1-\mu_0)^2 \tag{3}$$

$$\sigma_T^{2(th)} = \sum_{i=1}^{L-1} P_i(i-\mu_T)^2 \tag{4}$$

$$\mu_0 = \sum_{i=0}^{th} i\frac{P_i}{P_t} \tag{5}$$

$$\mu_1 = \sum_{i=th+1}^{L-1} i\frac{P_i}{1-P_t} \tag{6}$$

$$\mu_T = \mu_0 + \mu_1 \tag{7}$$

$$P_t = \sum_{i=0}^{th} P_i \tag{8}$$

$$1-P_t = \sum_{i=th+1}^{L-1} P_i \tag{9}$$

In the above equations, P_{th} denotes the probability of the grayscale level of the threshold pixel, μ_0 and μ_1 are the means of the first and second classes, and i represents the grayscale level.

A) Fractal dimension of binary sets

Let's take the Brodatz texture D5. From its histogram, we obtain the probability distribution function using equation 1. We search for the optimal threshold that maximizes the inter-class variance to total variance ratio given by equation 2. The box dimension used in this study is based on the box-counting method. After binarizing the grayscale levels, we count the number of boxes needed to cover the image, and then we plot the result on a bi-logarithmic plane. With a linear regression adjustment, we estimate the slope. This fractal attribute is given in Table 2 and represents the dimension of binary sets. The choice of analysis scales is important in discriminating between the 10 Brodatz textures, and we must use scales that are sufficiently fine ($\delta \rightarrow 0^+$).

B) Grayscale fractal dimension with differential box-counting in 3D

The relatively easy numerical implementation of this method has made it very famous. As its name suggests, it is based on counting the number of boxes needed to cover the object without overlap between the boxes. This covering can be done in at least five different ways, where $N_\delta(F)$ is the number of boxes of δ size that perfectly tile the object F. Thus, we can calculate the box dimension using the equation [5][16]:

$$\dim_B = \lim_{\delta \to 0} \frac{\log(N_\delta(F))}{-\log(\delta)} \tag{10}$$

First, we represent the texture as a rough surface in a 3D plane with the Z component indicating the gray level, and then we calculate the number of cubes with δ side that perfectly tile the resulting surface. In a bi-logarithmic plane, we plot the point cloud ($1/\delta$, $N_\delta(F)$), and the presence of linearity is an indicator of the fractal nature of the image. In fact, a wide variety of natural images exhibit scale invariance properties. To find the number of boxes required to tile an image of size [M×N], we grid the image with windows of size δ×δ, then we calculate Z_{max} and Z_{min} which correspond to the maximum and minimum intensities in the considered window, finally, the number of cubes required to tile the image is the sum of $\sum \left\lceil \frac{Z\max}{\delta} \right\rceil + \left\lfloor \frac{Z\min}{\delta} \right\rfloor$. using the symbol $\lceil\ \rceil$ to indicate the nearest upper integer and $\lfloor\ \rfloor$ the nearest lower integer, by sweeping the entire image without overlapping between the windows, the calculation results are given in table II.

C) Fractal lacunarity

It is used to describe the spatial distribution of voids (holes) in a fractal object. Indeed, some fractal structures have the same fractal dimension, so Mandelbrot introduced fractal lacunarity to address this problem. In this paper, the formula [3] [16] was used:

$$L(r) = \frac{V(r)}{M^2(r)} \tag{11}$$

with r representing the size of the box used in the calculation of the number of pixels, for example, L(1) refers to a box of 1 pixel, which gives the ratio of empty pixels to full pixels. For the natural textures of Brodatz, we opted for an interpolation using the sum of two exponential functions:

$$L(r) = a.\exp(b.r) + c.\exp(d.r) \tag{12}$$

This type of function significantly reduces the mean squared error when interpolating the fractal lacunarity curve, as shown in Table 2.

D) Fractal dimension by the area-perimeter relationship

To determine the Area-Perimeter dimension, let's consider the image after the binarization operation, which is in 2D. Let N_p and N_s be the numbers of boxes of size δ required to cover the perimeter and the area of the set of non-empty pixels, respectively. Then, the measured perimeter P and area A of this set are given by $P = N_p\delta$ and $A = N_s\delta^2$, respectively. The fractal dimension Area-Perimeter is obtained by fitting A as a function of P using linear regression in a bi-logarithmic plot [8] [16].

$$\frac{2}{D_B} = \lim_{\delta \to 0} \frac{\log A}{\log P} \quad (13)$$

E) Fractal dimension of contours

This dimension is obtained using the 2D box-counting method on the contours of the sets. The contours are detected after the binarization step. The contour detection step for binary images only requires a 2x2 window with zigzag scanning over the entire image. If the sum of the pixels inside the window is between 1 and 3, then the other pixels are forced to 1 (a pixel of the set = 1, and 0 for the void). The pixels thus found represent contour pixels. Table 2 illustrates the results found.

F) Power spectrum exponent fractal dimension of binary sets

Power spectrum analysis has been successfully applied in the study of precipitation data variations, temperature variations, oceanic flux measurement, Nile river flooding, stock market prices, EGG signals in physiology, electromagnetic fluctuations through superconductors, analysis of electronic component noise, terrain texture variations, cloud formation, etc. [24]. A wide range of natural phenomena and real-world signals exhibit a behavior known as "1/f," a relationship that holds over a broad range of frequencies f. These types of processes have a power spectrum that follows a power law of the form [16][24][25]:

$$S_x(\omega) \approx \frac{\Gamma_x^2}{|\omega|^\beta} \quad (14)$$

The parameter β is related to H, the Hurst exponent, through the equation β = 2H + 1, and Γ_x^2 represents the power spectral density. For any statistically self-similar random process x(t), it can be approximated by : $x(t) \approx a^{-H} x(at)$ whatever the real $a > 0$ and the time parameter $-\infty < t < +\infty$.

We must take into account the constraint related to the size of the data. This implies excluding parts of the spectrum belonging to low and high frequency regions due to poor resolution. In certain cases, such as for fBm (fractional Brownian motion) signals, where 1 < B < 3, the fractal dimension Df is related to the parameter H according to the expression:

$$D_f = 2 - H \quad (15)$$

We have calculated the power spectrum exponent for different regions of interest in satellite image (see Table. II).

III. MULTILAYER PERCEPTRON

The MLP is arguably the most popular among Artificial Neural Networks ANNs. In this model, multiple inputs correspond to fractal attributes, as in our case, and it produces different image classes as output. The MLP is primarily composed of three layers: the input layer, the output layer, and one or more hidden layers (see Fig.1) [26][27]. In this neural network, the backpropagation technique is used for training the network, based on the relationship:

$$y = \varphi(\sum_{i=1}^{n} w_i x_i + b) = \varphi(w^T x + b) \quad (16)$$

With φ as the activation function, w and x denoting the weight and input vectors, and b as the bias.

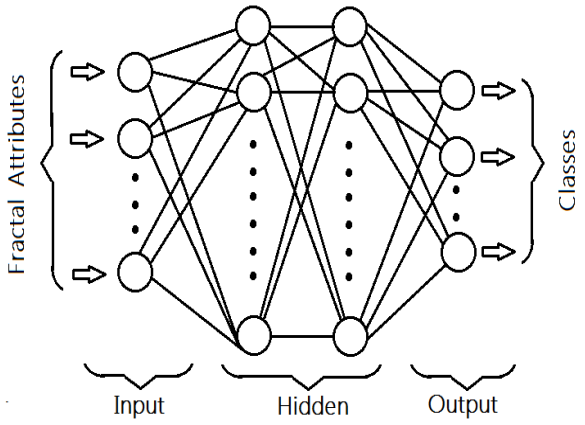

Fig. 1. MLP with fractal attributes as inputs and different image classes as outputs.

IV. SATELLITE DATABASE

To evaluate the effectiveness of our investigation,we have chosen a number of regions of interest, including agricultural, urban, forested, mountainous, water-dammed, and even cloud-covered areas. These areas were captured by the Landsat-8 satellite obtained from [28] through the Landsat Explorer interface. Only

bands (2, 3, 4, and 5) corresponding to the Red, Green, Blue, and NIR bands with a resolution of 30 meters have been used in this work out of the eleven bands delivered by the Landsat-8 satellite. The GPS coordinates of the polygon (1.858034; 37.093868)-(3.93878; 36.698338)-(3.414576; 34.979166)-(1.382512; 35.372636), centered at (2; 36), delineate the location of the obtained image, which was taken on May 6, 2017.

For this purpose, we have taken into consideration three different parts of the chosen image, each measuring 15 km by 15 km and 500 x 500 pixels. The GPS coordinates at the centers are (2.78498; 36.57439), (2.92461; 36.66384), and (2.83408; 36.40132), corresponding respectivelyto agricultural land and urban areas (Part 1) (Fig. 2), dams in urban areas (Part 2) (Fig.3), and mountains and clouds with urban areas (Part 3) (Fig.4).

Fig. 2. Image showing RGB and NDVI for the coordinate center (2.78498, 36.57439) using Google Earth Engine.

Fig. 3. Image showing RGB and NDVI for the coordinate center (2.92461, 36.66384) using Google Earth Engine.

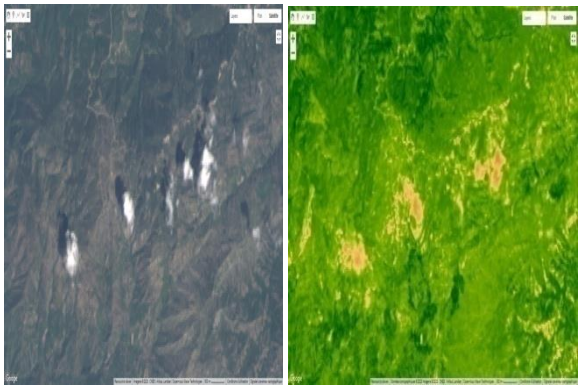

Fig. 4. Image showing RGB and NDVI for the coordinate center (2.83408, 36.40132) using Google Earth Engine.

We include in our analysis the same fractal attributes tested on the Brodatz textures, namely: the fractal dimension DBC, the fractal lacunarity, the fractal dimension of the contours of the binary image using the Otsu method, the fractal dimension of the sets of the binary image, the area-perimeter dimension, and the power spectrum exponent. We analyzed the RGB bands using the different fractal attributes, using the [29] formula to convert them to grayscale.

$$I = 0.2989 \times R + 0.5870 \times G + 0.1140 \times B \quad (17)$$

To calculate the NDVI using the NIR and RED bands, we use the following formula [30]:

$$NDVI = (NIR - RED)/(NIR + RED) \quad (18)$$

V. COMBINATIONS OF PARAMETERS FOR CLASSIFICATION

Let A_n represent the fractal attributes calculated with $n \in N$ and $1 \leq n \leq 6$, in the following order: (n=1) binary set dimension, (n=2) dimension of gray intensity considered as rough surface, (n=3) parameter b obtained by interpolating the fractal lacunarity curve, (n=4) area-perimeter dimension, (n=5) contour dimension, and (n = 6) power spectrum exponent β.

In order to evaluate the dispersion, we have opted for an analysis of variance, thus for a given combination of attributes:

$$comb_i = \sum_{n=1}^{6} 2^{P_n} \quad (19)$$

where $P_n = 1$ if An is chosen in the combination, and Pn = 0 if the attribute An is not chosen. In this paper, the number of parameters is N = 6, so we have 2N-1 possible combinations with $1 \leq i \leq 63$ in the calculation of the variance of combination with index i:

$$\mathrm{var}_i = \mathrm{var}_{1\leq m\leq 10}\left(\sqrt{\sum_{n=1}^{N} P_n\left(A_{n,m} - \overline{A_n}\right)^2}\right) \quad (20)$$

Var: denotes the variance, m indicates the Brodatz texture with $1 \leq m \leq 10$, $A_{n,m}$ represents the fractal attribute n of texture m.

$$\overline{A_n} = \frac{1}{N}\sum_{m=1}^{N} A_{n,m} \quad (21)$$

gives the average of attribute n for the N textures used. It is important to note that the data should be standardized before calculating the variance (see Fig.5).

VI. RESULTS AND DISCUSSION

Case of Brodatz textures: After the analysis of variance, the table.I presents the combinations of attributes that exhibit the highest dispersions, as well as those that yield the lowest dispersions:

With these preliminary results, the combination based on the use of the texture after binarization yields very satisfactory results and exhibits higher variance compared to other combinations (see combi=25 in the table). It even surpasses the variance of fractal attributes from conventional methods (combi = 32,4,2).

Therefore, it is necessary to expand our analysis to the entire natural Brodatz texture database and propose other approaches for measuring dispersion.

We are looking to find the best combination to achieve the highest dispersion among the fractal attributes, which means greater discrimination between the distinguished regions of interest. Thus, we used four different regions representing agricultural areas, urban regions, forested regions, and mountainous regions.

Case of Satellite Database : Initially, we normalized the seven attributes (Fig.5). We additionally incorporated the fractal dimension via DBC of NDVI, treated as a surface, to the six attributes utilized with the Brodatz textures. Subsequently, through experimentation with different combinations, we pinpointed the optimal combination, which, as depicted, consists of the Area-Perimeter Dimension, Fractal Contour Dimension, and Fractal Dimension by DBC of NDVI (Fig.6).

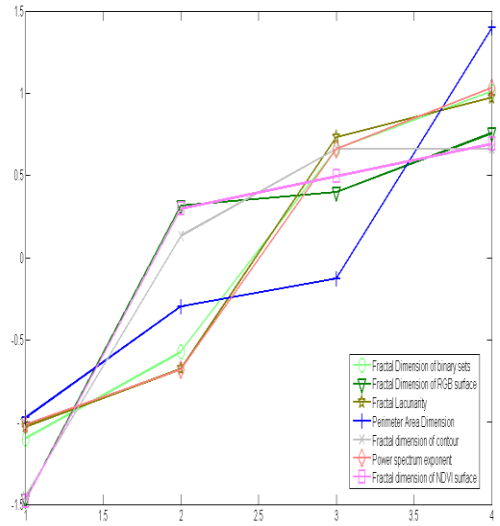

Fig. 5. Normalized fractal attributes for four different regions of the Landsat-8 satellite image.

$Comb_i$	25	27	29	9	31	2	48
P_1	1	1	1	1	1	0	0
P_2	0	1	0	0	1	1	0
P_3	0	0	1	0	1	0	0
P_4	1	1	1	1	1	0	0
P_5	1	1	1	0	1	0	1
P_6	0	0	0	0	0	0	1
var_i	0.971	0.961	0.939	0.925	0.924	0.244	0.234

TABLE I

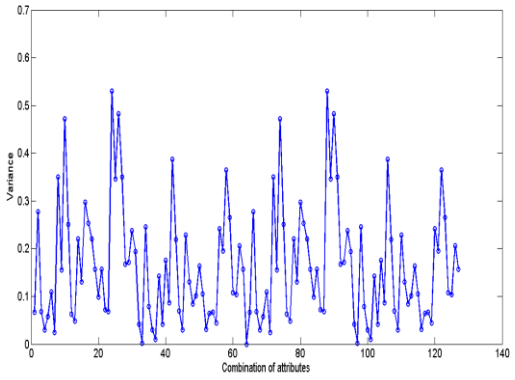

Fig. 6. Calculation of variance for all possible combinations of fractal attributes for the four regions of the Landsat-8 image.

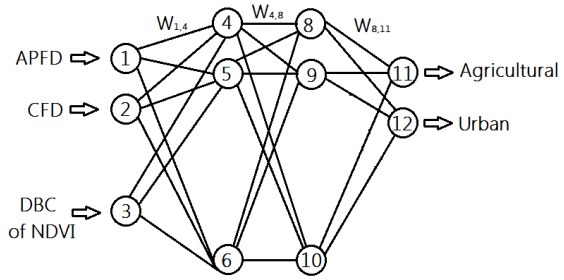

Fig. 7. The MLP with three inputs, two outputs, and two hidden layers.

According to Fig.6, the best combination is represented by 88, which corresponds to 1011000. Therefore, we should choose the fractal attributes: Area-Perimeter Fractal Dimension of RGB, Contour Fractal Dimension, and Fractal Dimension of NDVI surface. Indeed, this combination yields the highest dispersion among the four different regions of interest, which have distinct natures. By using this combination as the input to the neural network, and an architecture consisting of two hidden layers, each with three neurons (see Fig.7), As the activation function, we used the sigmoid, given by:

$$g(u) = \frac{1}{1+e^{-u}} \tag{22}$$

The total number of epochs is 6047 with a mean square error of 0.0066273, we achieved an accuracy of 100%, a recall of 87.5%, and an F1 score of 93.33%. In training our neural network, we used only the first two images from (part 1 in Table II, see Fig.8) of agricultural and urban terrain. Out of the 16 different image sections we processed, we obtained only 2 incorrect results (where two agricultural regions are detected as urban).

VII. CONCLUSION

Fractal attributes have shown great potential in texture classification and segmentation. In this work, we proposed the introduction of additional fractal parameters, such as the fractal dimension of contours and the fractal dimension of sets after image binarization using the Otsu method. We also utilized the Area-Perimeter dimension on the binarized image.

The evaluation of dispersion using variance demonstrated the ability of fractal attributes to discriminate among the 10 Brodatz textures, despite the loss of information due to data reduction. Preliminary results even indicate superiority compared to conventional methods such as differential box-counting of grayscale intensities, fractal lacunarity, and spectral analysis. It is also worth noting that processing binary images allows for reduced analysis and processing time.

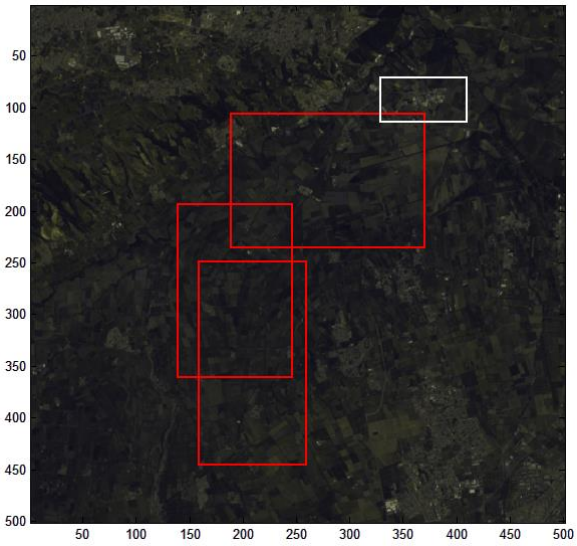

Fig. 8. Illustration of the regions selected in the training and testing of the MLP from image part 1, with agricultural areas in red and the urban region in white.

Similar to the case of Brodatz textures, we observe that the combination using the area-perimeter dimension and contour dimension demonstrated significant promise in classification. Furthermore, incorporating the fractal dimension of the NDVI surface has enhanced the discrimination among images from distinct classes. Through the utilization of the multilayer neural network, we achieved an accuracy of 100%, a recall of 87.5%, and an F1 score of 93.33%.

In addition, the use of low-resolution multispectral images, combined with deep learning techniques, offers a valuable tool for detecting agricultural and urban lands, monitoring irrigation, and evaluating food security. It provides essential data for decision-making in agriculture, urban planning, and natural resource management, contributing to more effective and sustainable environmental management.

VIII. REFERENCES

[1] Klonowski W., 2000 : *Signal and pattern analysis using Chaos theory and Fractal geometry*. Polish academy of sciences. p. 31.

[2] GAO, Qiuya, WEN, Tao, et DENG, Yong. Information volume fractal dimension. *Fractals*, 2021, *vol. 29, no 08*, p. 215-263.

[3] Bandt C., S. Graf and M. Zahle, 1995 : *Fractal Geometry and Stochastics*, Progress in Probability. Birkhauser Verlag.

[4] WANG, Yupin, LI, Xiaodi, WANG, Da, et al. A brief note on fractal dynamics of fractional Mandelbrot sets. *Applied Mathematics and Computation*, 2022, *vol. 432*, p. 127-353.

[5] Falconer K., 2003 : *Fractal Geometry : Mathematical Foundations and Applications*, 2nd Edition. John Wiley and Sons. 328 p.

[6] ZHANG, Yu-Dong, CHEN, Xian-Qing, ZHAN, Tian-Ming, et al. Fractal dimension estimation for developing pathological brain detection system based on Minkowski-Bouligand method. *IEEE Access*, 2016, *vol. 4*, p.5937-5947.

[7] Liebovitch L.S., 1998 : *Fractals and Chaos simplified for the life sciences*. Oxford University Press.

[8] Addison P. S., 1997 : *Fractals and Chaos An Illustrated Course*. Institute of Physics Publishing, Bristol and Philadelphia.

[9] FLORIO, Brendan J., FAWELL, Phillip D., et SMALL, Michael. The use of the perimeter-area method to calculate the fractal dimension of aggregates. *Powder technology*, 2019, *vol. 343*, p. 551-559.

[10] Sander E., L.M. Sander and R.M. Ziff, 1994 : Fractals and Fractal Correlation. *Computers in Physics, 8, 420.*

[11] S. OURABIA & Y. SMARA, 2016. A New Pansharpening Approach Based on Nonsubsampled Contourlet Transform Using Enhanced PCA Applied to SPOT and ALSAT-2A Satellite Images. *Journal of the Indian Society of Remote Sensing 44 (5), 665-674*. DOI 10.1007/s12524-016-0554-9, Print ISSN 0255-660X, Online ISSN0974-3006.

[12] S. Ourabia, N. Baaziz, Y. Smara, Pansharpening Methods Based on a Redundant Contourlet Transform, *2023 International Conference on Earth Observation and Geo-Spatial Information* (ICEOGI) | 979-8-3503-9672-0/23/$31.00 ©2023 IEEE | DOI: 10.1109/ICEOGI57454.2023.10292972

[13] SULIMAN, Alaeldin et ZHANG, Yun. A review on back-propagation neural networks in the application of remote sensing image classification. *Journal of Earth Science and Engineering*, 2015, *vol. 5, no 1*, p. 52-65.

[14] KHIDER, Mohamed, TALEB-AHMED, Abdelmalik, DUBOIS, Patrick, et al. Classification of trabecular bone texture from MRI and CT scan images by multi resolution analysis. *In : 2007 29th Annual International Conference of the IEEE Engineering in Medicine and Biology Society*. *IEEE*, 2007. p. 5589-5592.

[15] KHIDER, Mohamed, HADDAD, Boualem, et AHMED, Abdelmalik Taleb. Multifractal analysis by the large deviation spectrum to detect osteoporosis. *In : 2013 8th International Workshop on Systems, Signal Processing and their Applications (WoSSPA). IEEE*, 2013. p. 112-115.

[16] KHIDER, Mohamed. *Analyse multifractale par MMTO-2D: Évaluation sur des images radar et médicales.* 2011. Thèse de doctorat. thèse de Doctorat en électronique, Université des Sciences et de la Technologie Houari Boumediene USTHB.

[17] KHIDER, Mohamed, HARRAR, Khaled, JENNANE, Rachid, et al. Texture Analysis: A comparison between Multifractal Spectrum with Legendre Transform and the Box-Counting Method. 2013.

[18] E. Charou et al., "Deep Learning for Agricultural Land Detection in Insular Areas," 2019 *10th International Conference on Information, Intelligence, Systems and Applications (IISA)*, Patras, Greece, 2019, pp. 1-4.

[19] KAPUR J.N., P.K. SAHOO, A.C.K. Wong A new method for graylevelPicture thresholding using the entropy of the histogram, *Computer Vision, Graphics and Image Processing, Vol. 29*, 1985. pp. 273-285.

[20] YOUSEFI, Jamileh. Image binarization using Otsu thresholding algorithm. Ontario, Canada: University of Guelph, 2011, *vol. 10*.

[21] TRUSSEL J. Comments on Picture thresholding using an iterative selection method. *IEEE Trans.Syst. Manage. Cybern. (SMC) 9: 311*.(1979).

[22] ZHOU, Donghua. Bus Passenger Recognition and Track of Video Sequence. *Journal of Multimedia*, 2013, *vol. 8, no 3*.

[23] CHAKI, Nabendu, SHAIKH, Soharab Hossain, SAEED, Khalid, et al. A comprehensive survey on image binarization techniques. *Springer India*, 2014.

[24] Wornell G., 1996 : *Signal processing with fractals: a wavelet-based approach*. Prentice Hall Press Upper Saddle River, NJ, USA. 177 p.

[25] RANGAYYAN, Rangaraj M., OLOUMI, Faraz, WU, Yunfeng, et al. Fractal analysis of knee-joint vibroarthrographic signals via power spectral analysis. *Biomedical Signal Processing and Control*, 2013, *vol. 8, no 1*, p. 23-29.

[26] Rosenblatt, F. (1962). *Principles of neurodynamics: Perceptrons and the theory of brain mechanisms*. Spartan Books, Washington DC, 1962.

[27] SALAH, Mahmoud. A survey of modern classification techniques in remote sensing for improved image classification. *Journal of Geomatics*, 2017, *vol. 11, no 1*, p. 21.

[28] Pettorelli, Nathalie, Vik, Jon Olav, Mysterud, Atle, et al. Using the satellite-derived NDVI to assess ecological responses to environmental change. *Trends in ecology & evolution*, 2005, *vol. 20, no 9*, p. 503-510.